A Fast Algebraic Estimator for System Parameter Estimation and Online Controller Tuning - A Nanopositioning Application

***Abstract*—Parameter uncertainty is a key challenge in the real-time control of nanopositioners employed in Scanning Probe Microscopy. Changes in the sample to be scanned, introduces changes in system resonances; requiring instantaneous online tuning of controller parameters to ensure stable, optimal scanning performance. This paper presents a method based on the frequency-domain algebraic derivative approach for the accurate online identification of the nanopositioner's parameters. The parameter estimates are produced within a fraction of one period of the resonant mode frequency, allowing almost instantaneous tuning of controller parameters. Experimental results show that the proposed method can be utilized to automatically tune an Integral Resonant Control (IRC) scheme, that combines both damping and tracking actions, and consequently deliver positioning performance far superior to that achieved solely due to the scheme's inherent robustness properties. It is further shown that the achieved performance compares favourably with an optimally designed control scheme of the same type.**

***Index Terms*—Nanopositioning, Algebraic Parameter Estimation, Integral Resonant Control.**

I. Introduction

HIGH-SPEED NANOPOSITIONING is a key enabler in several scientific areas such as biotechnology [1], [2], fibre optics [3], medicine [4], sensing [5] etc. Piezoelectric-stack driven nanopositioners have gained high popularity in recent years, [6] due to their numerous advantages such as mechanical robustness, relatively large travel ranges, high resolution, repeatability, accuracy and absence of friction or stiction. The resonant dynamics of these nanopositioners, combined with the nonlinear effects induced by the piezoelectric actuators, i.e., hysteresis and creep, mandate the design and implementation of an effective closed-loop control scheme to achieve accurate positioning performance. Consequently, most popular control schemes incorporate both damping (for the mechanical resonances) and tracking (for accurate positioning) actions, [7].

During active scanning operations, changes in resonant frequency by up to 80%, can be introduced by numerous factors. Some of these changes can be estimated to a certain extent - for example: changes in the mass of the sample scanned, additional mass introduced by heating elements, magnetic coils or liquid cells etc. On the other hand, changes in the temperature, humidity, payload during pick and place tasks at nanometric scale, tribology variations etc., are difficult to predict [8]. This uncertainty in key system parameters makes it extremely difficult to design effective controllers, as most control design techniques (and performance thereof) are based on an accurate system model, [9]. Till date, this parameter uncertainty was addressed by ascertaining that the designed control scheme was robust to parameter variations within a certain operational limit. Consequently, several control techniques that possess adequate robustness have been proposed, [10], [11], [12], [13], [14], [15]. These techniques, though robust, undergo considerable degradation in positioning performance when the system moves away from the nominal model parameters on which the controller design was initially based. This is why many commercial nanopositioners define a limited range of admissible payloads (changes in mass results in subsequent changes in resonant frequency) and indicate the maximum scanning frequency associated with each mass, for which the nanopositioners deliver acceptable positioning performance.

To overcome this limitation, this paper applies the general algebraic framework for linear identification proposed in [16], to formulate a specific algorithm aimed at the online parameter estimation of a lightly damped second order systems, hitherto not addressed in literature. Furthermore, a new re-initiation algorithm is also proposed. Though several re-initiation algorithms have been published in literature, arguably the more efficient one was reported in [17]. The re-initiation algorithm proposed in this paper, outperforms the one presented in [17] by: 1) Requiring less computational effort and computer memory and 2) Ensuring smooth convergence to zero, thereby yielding parameter estimates in less time (typically shorter than one period of the resonance frequency). Moreover, previous works [18] and [19] identified only two parameters of slowly oscillating systems (the resonance frequencies were under 2 Hz). The algorithm proposed in this paper is capable of identifying three parameters of significantly fast oscillating system (resonance frequency $>$700 Hz) in less than one period of the resonance frequency, using relatively low sampling rates and limited computation capabilities. The proposed estimator is especially well-suited to track step-wise changes in system parameters such as those introduced by the addition or removal of mass (effected by changes in the scanned sample) on the nanopositioner. These estimates can further be utilized to automatically tune a multitude of popular control schemes applied to nanopositioners. Due to it's simplicity, inherent robustness, good performance and guaranteed stability, the Integral Resonant Control (IRC) scheme that combines both damping and tracking actions, [12], has been chosen as a candidate to demonstrate the efficacy of the proposed algebraic estimation and re-initiation algorithm.

This paper is organized as follows. Section II formally states

the problem and presents the algebraic estimation scheme utilized in this work. The experimental setup is described in Section III. Simulated as well as real-time experimental results that validate the proposed algebraic estimator are presented and discussed in Section IV. Section V concludes the paper.

II. Problem Statement and Background Theory

The frequency-response of one axis of a typical nanopositioner exhibits a dominant lowly-damped resonant peak and can be modeled with good accuracy, as a lightly-damped mass-spring-damper system whose dynamics can be described by:

$$\ddot{y}(t) + 2\zeta\omega_n\dot{y}(t) + \omega_n^2 y(t) = \sigma^2 u(t) \tag{1}$$

where $y(t)$ is the displacement of the moving platform, $u(t)$ is the input voltage applied to the actuator, σ^2 corresponds to the equivalent stiffness of the mechanism, ζ is the damping coefficient, and ω_n is the natural frequency of vibration of the system, [20]. To initiate any control design, the system parameters σ, ζ, and ω_n need to be estimated accurately from $u(t)$ and $y(t)$. These system parameters are often time-variant. Furthermore, these estimated parameters are often utilized to tune a controller in an adaptive control scheme. Thus, the desirable features for an appropriate estimation algorithm are:

1) Short estimation time: The time required to generate an accurate estimate must be shorter than one period of the targeted resonant mode frequency. This will enable quick tuning of the controller parameters without long periods of sub-par performance due to an incorrectly tuned controller. Since the nanopositioner used in the experiments to verify this work exhibits its first resonant mode at ≈700 Hz, an estimation time of the order of 1 ms is required.
2) Robustness to unmodeled dynamics: The system is modeled as a second-order resonant system, yet, as seen in Section III, at least four high-frequency resonant modes can be seen in the recorded frequency response for the nanopositioner axis. As the frequency of the second mode is less than two times the frequency of the first mode, it is apparent that the second mode will have a clear impact on the output signal and can potentially introduce errors in any system parameters identified based on a single resonant-mode model.
3) Practicality and Applicability: The algorithm should be implementable on a standard PC with modest computation capabilities and be relatively insensitive to coarse sampling. Furthermore, the identification algorithm must be relatively simple in order to facilitate real-time implementation. For the system used to conduct experiments reported in Section III, the sampling rate is about 30 KSs^{-1}. Therefore, each period of the first resonant mode is characterized by only 30-40 samples (and a significantly less number of samples characterize the higher modes).

Phase-locked-loop (PLL) topologies [21], adaptive notch filters [22], robust globally convergent estimators [23], continuous least squares [24], frequency-locked-loop filters [25] and Prony-based methods [26] have all been applied to estimate the parameters of undamped resonant modes. However, these methods show high sensitivity to noise as well as the neglected high-frequency modes and in most instances, are incapable of providing good estimates for systems with lightly damped resonant modes, typical of nanopositioner axes. Additionally, these methods require time equivalent to several periods of the resonant frequency to generate an accurate estimate of the system parameters. All these drawbacks are overcome by algebraic estimators [27], [28]. Continuous transfer functions have also been obtained using algebraic identification techniques, having mainly been applied to electrical drives [29], [30]. It was shown in [31], that algebraic identification methods converge to accurate estimates in significantly less time compared to algorithms based on discrete least squares. Moreover, algebraic identification techniques are based on relatively simple algorithms that can be easily implemented in real-time, and possess low sensitivity to slow sampling rates.

As the algebraic identification technique possesses all the desirable features listed earlier, it emerges as the most appropriate approach to be applied to parameter identification and controller tuning for nanopositioning applications.

A. Estimation algorithm

The Laplace transform of the equation of motion of the a single mass-spring-damper system presented in (1), is given by:

$$\begin{aligned}\sigma^2 U(s) =& s^2 Y(s) - sy(0) - \dot{y}(0) \\ &+2\zeta\omega_n\left[sY(s) - y(0)\right] + \omega_n^2 Y(s)\end{aligned} \tag{2}$$

where Y and U are the Laplace transforms of $y(t)$ and $u(t)$ respectively. Double differentiation with respect to the complex variable "s", cancels the initial conditions.

$$\begin{aligned}\frac{\partial^2 U}{\partial s^2} =& \frac{1}{\sigma^2}\left[2Y + 4s\frac{\partial Y}{\partial s} + s^2\frac{\partial^2 Y}{\partial s^2}\right] \\ &+\frac{2\zeta\omega_n}{\sigma^2}\left[2\frac{\partial Y}{\partial s} + s\frac{\partial^2 Y}{\partial s^2}\right] + \frac{\omega_n^2}{\sigma^2}\frac{\partial^2 Y}{\partial s^2}\end{aligned} \tag{3}$$

In order to avoid multiplications by positive powers of s, which are translated as undesirable time derivatives in the time-domain, we multiply (3) by s^{-2}. Rearranging this expression, we obtain:

$$\begin{aligned}s^{-2}\frac{\partial^2 U}{\partial s} =& \frac{1}{\sigma^2}\left[2Ys^{-2} + 4s^{-1}\frac{\partial Y}{\partial s} + \frac{\partial^2 Y}{\partial s^2}\right] \\ &+\frac{2\zeta\omega_n}{\sigma^2}\left[2s^{-2}\frac{\partial Y}{\partial s} + s^{-1}\frac{\partial^2 Y}{\partial s^2}\right] \\ &+s^{-2}\frac{\omega_n^2}{\sigma^2}\frac{\partial^2 Y}{\partial s^2}\end{aligned} \tag{4}$$

Let $\mathcal{L}$ denote the usual operational calculus transform acting on exponentially bounded signals with bounded left support [32]. Recall that $\mathcal{L}^{-1}s(\cdot) = d/dt(\cdot)$, $\mathcal{L}^{-1}1/s(\cdot) = \int_0^t(\cdot)(\sigma)d\sigma$, and $\mathcal{L}^{-1}d^v/ds^v(\cdot) = (-1)^v t^v(\cdot)$. Expression (4) can thus be written in the time-domain as follows:

$$\int^2 t^2 u = \frac{1}{\sigma^2}\left[2\int^2 y - 4\int ty + t^2 y\right] + \frac{2\zeta\omega_n}{\sigma^2}\left[-2\int^2 ty + \int t^2 y\right] + \frac{\omega_n^2}{\sigma^2}\int^2 t^2 y \quad (5)$$

Expression (5) can be written in a compact form as:

$$q(t) = \frac{1}{\sigma^2}\beta(t) + \frac{2\zeta\omega_n}{\sigma^2}\xi(t) + \frac{\omega_n^2}{\sigma^2}\eta(t) \quad (6)$$

where $q(t)$, $\beta(t)$, $\xi(t)$, and $\eta(t)$ can be calculated in real-time as they are the outputs of the following time-varying linear unstable filters:

$$\begin{array}{llll} q(t) = z_1 & \beta = z_3 + t^2 y & \xi = z_5 & \eta = z_7 \\ \dot{z_1} = z_2 & \dot{z_3} = z_4 - 4ty & \dot{z_5} = z_6 + t^2 y & \dot{z_7} = z_8 \\ \dot{z_2} = t^2 u & \dot{z_4} = 2y & \dot{z_6} = -2ty & \dot{z_8} = t^2 y \end{array} \quad (7)$$

whose initial states are set to zero.

The linear equation (6) has three unknowns, σ, ζ and ω_n, which can be obtained from a least-squares error fitting in the time interval $[t_i, t_f]$ (where the interval $[t_i, t_f]$ is equal to the interval of time between the first and the last available sample). With a change of variables such that:

$$A = \frac{1}{\sigma^2}, B = \frac{2\zeta\omega_n}{\sigma^2}, C = \frac{\omega_n^2}{\sigma^2}, \quad (8)$$

a cost function can be defined as:

$$\varepsilon = \int_{t_i}^{t_f} \left\{ \begin{bmatrix} \beta(\tau) & \xi(\tau) & \eta(\tau) \end{bmatrix} \cdot \begin{bmatrix} A \\ B \\ C \end{bmatrix} - q(\tau) \right\}^2 d\tau, \quad (9)$$

The minimization of this cost function leads to:

$$\begin{bmatrix} A \\ B \\ C \end{bmatrix} = \left[\int_{t_i}^{t_f} \begin{bmatrix} \beta(\tau) \\ \xi(\tau) \\ \eta(\tau) \end{bmatrix} \cdot \begin{bmatrix} \beta(\tau) & \xi(\tau) & \eta(\tau) \end{bmatrix} d\tau\right]^{-1} \cdot \int_{t_i}^{t_f} \begin{bmatrix} \beta(\tau) \\ \xi(\tau) \\ \eta(\tau) \end{bmatrix} q(\tau) d\tau \quad (10)$$

The batch formula expressed in (10), was first applied for algebraic parameter estimation in [29]. Furthermore, a recursive formula of the least-squares algorithm that demonstrated increased computational efficiency, was used in [30] to estimate the parameters of a DC motor using an algebraic estimator. The parameters σ, ζ and ω_n are only weakly linearly identifiable. This signifies that once A, B and C have been identified, σ, ζ and ω_n can be easily determined by using the following non-linear relations:

$$\sigma = \frac{1}{\sqrt{A}}, \qquad \zeta = B\sqrt{\frac{1}{4AC}}, \qquad \text{and} \qquad \omega_n = \sqrt{\frac{C}{A}} \quad (11)$$

B. Re-initiation Algorithm

In order to perform the online estimation of the nanopositioner parameters, it is necessary to reset and re-initiate the aforementioned algorithm because: 1) linear time-varying filters are unstable, and the values of the variables involved in the estimation may therefore become very large as time increases and 2) the noise present in the measurements may produce wrong estimates such as negative values for σ, ζ and ω_n. To avoid these issues, it is important to have a criterion which clearly discriminates between two cases: 1) the estimator is providing good estimates and the procedure has converged to meaningful close-to-actual estimates of the parameters and 2) the samples utilized to produce the estimates cannot converge and it is necessary to re-initiate the estimation algorithm.

In order to determine the time of re-initiation, [17] proposed a criterion based on the moving average and on the moving standard deviation of the estimates of frequency. However, these operations require the storage of a relatively high number of samples that comprise the moving window that is utilized to perform the average and the standard deviation. It is important to note that even if the recursive implementation of these operations is performed, all the samples need to be stored in a circular array. This may cause issues if the system presents limited memory or if it takes a long time to displace all the samples through the circular array.

To overcome the aforementioned issues and to utilize a more computationally efficient approach, the proposed procedure is based on the Exponentially Weighted Moving Average (EWMA) and the Exponentially Weighted Moving Standard Deviation (EWMSTD) [33]. These two operators are commonly employed in forecasting seasonals and trends in economics. However, to the best of the authors' knowledge, this is the first time this criterion is used to define the re-initiation procedure of an algebraic estimator. The recursive formulae of the EWMA and the EWMSTD are given below:

$$Z(i) = \lambda_1 \cdot X(i) + (1 - \lambda_1) Z(i-1), \quad (12)$$

and:

$$S(i) = \sqrt{\lambda_2 (X(i) - Z(i))^2 + (1 - \lambda_2) S^2(i-1)} \quad (13)$$

where $Z(i)$ is the EWMA computed for the i^{th} sample $X(i)$, $S(i)$ is the i^{th} EWMSTD computed for the i^{th} sample $X(i)$, and λ_j, $0 < \lambda_j \leq 1$, $j = 1, 2$ are two smoothing constants. In both cases, the initialization values are defined as $Z(1) = X(1)$ and $S(1) = X(1)$. It is important to note that from a control point of view, the EWMA is just a different representation of the Discrete Euler Backward implementation of a first-order low-pass filter. By using these definitions and the outputs of the algebraic estimator provided by (11), it can be concluded that the estimation has converged when the condition:

$$\frac{S_{\omega_n}(n)}{|Z_{\omega_n}(n)|} \leq \delta \quad \cap \quad Z_\sigma(n) > 0 \quad \cap \quad Z_\zeta(n) > 0 \quad (14)$$

is verified. $S_{\omega_n}(n)$ and $Z_{\omega_n}(n)$ are the standard deviation and the average value of the estimated natural frequency of the system computed by using the EWMA and the EWMSTD. δ is the tolerance parameter that determines the accuracy of the estimate of the natural frequency of the system. Additionally, conditions $Z_\sigma(n) > 0$ and $Z_\zeta(n) > 0$ are imposed to ensure $\sigma > 0$ and $\zeta > 0$. Considering T_s to be the sampling time, the sample under which condition (14) is verified is denoted as $\hat{n}$, and the time $\hat{n} \cdot T_s$ is the operation time interval corresponding to the interval of time from the beginning of the estimation process (it is assumed that $n = 0$ when the estimation starts) until (14) is satisfied. The estimates provided by the algorithm are:

$$\omega_n^e = Z_{\omega_n}(\hat{n}), \qquad \sigma^e = Z_\sigma(\hat{n}), \qquad \zeta^e = Z_\zeta(\hat{n}), \qquad (15)$$

If condition (14) is not verified after time T_r, the resulting estimates are deemed invalid and the algorithm is re-initiated. The selection of T_r is based on experience: a good compromise is often that of choosing a value of the order of the period of the lowest frequency that has to be estimated.

The proposed real-time estimation algorithm can be summarized as follows:

1) Initiate the algorithm.
2) During each sampling period, use inputs of the Brunovsky filter (7), i.e. the voltage applied to the system u, the displacement of the nanopositioner y, and the time t as input to the estimator and compute new estimates of system parameters (ω_n, σ, and ζ) using (10) and (11).
3) Compute (12), (13) using successive estimates of ω_n σ, and ζ.
4) Check the re-initiation criterion (14). If this criterion is verified, the last value of each EWMA will be considered a valid estimation of the system parameters (15). If a time T_r is reached and (14) is not fulfilled, return to step 1).

In the next section, a brief description of the experimental setup employed to validate the efficacy of the proposed algorithm is presented, followed by both simulation and experimental results.

III. Experimental Setup

The experimental setup pictured in Fig. 1, consists of a flexure-based XY serial-kinematic nanopositioner, voltage amplifiers and displacement sensors. The nanopositioner is driven by two piezoelectric-stacks, each with a stroke of $\pm$ 20 μm. The nanopositioner delivers translational motions along x and y axes which are measured by a Microsense 4810 capacitive displacement sensor and a 2805 measurement probe with a measurement range of $\pm$ 50 μm for a corresponding voltage output of $\pm$ 10 V. All experimental data is recorded in real-time, using a PC OPTIPLEX 780 with an Intel(R) Core(TM)2 Duo Processor running at 3.167 GHz and equipped with 2GB of DDR3 RAM memory. The whole system is capable of deterministic sampling times as low as 30 μs. In order to interface between the nanopositioner and the PC, a PCI-6621 data acquisition card from National Instruments installed on a second PC running the Real-Time Module from LabVIEW is utilized.

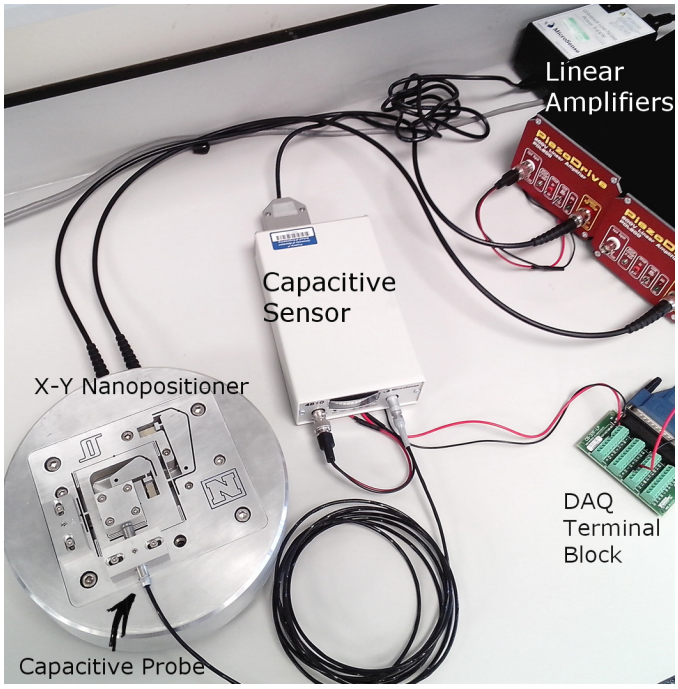

Fig. 1. A two-axis serial kinematic nanopositioner, designed at the EasyLab, University of Nevada, Reno.

In order to characterize the dynamics of the nanopositioner, small signal frequency response functions (FRFs) were recorded. The FRFs are obtained by applying a sinusoidal chirp signal (from 10 Hz to 1800 Hz) with an amplitude of 0.2 V as input to the voltage amplifier of the $x-$axis and measuring the output signal (sensor voltage proportional to axial displacement) along the same axis. Subsequently, the FRF is computed by taking the Fourier transform of the recorded data. The same procedure was repeated for obtaining the $y-$axis FRF. It is important to note that since the capacitive sensor measures relative displacements from a zero point, before each experiment a new zero point is measured in order to avoid any offset in the measurements. In Figure 2, the magnitude responses of the two axes of the nanopositioner are plotted (recorded using a sampling time of 50 μs).

The chosen frequency range captures the dominant resonant mode of the nanopositioner as well as a number of high-frequency secondary modes that can be neglected due to their low dynamic range when compared to the first dominant resonant mode. The identified transfer function parameters for both axes of the nanopositioner are given in Table I.
It is also important to note that the parameters of the system used in (1) correspond to the dominant first resonant mode of the corresponding axis as reported in Table I.

IV. Real-time parameter estimation of a nanopositioner

The proposed algebraic estimator involves two algorithms: the estimation procedure and the convergence criterion. In

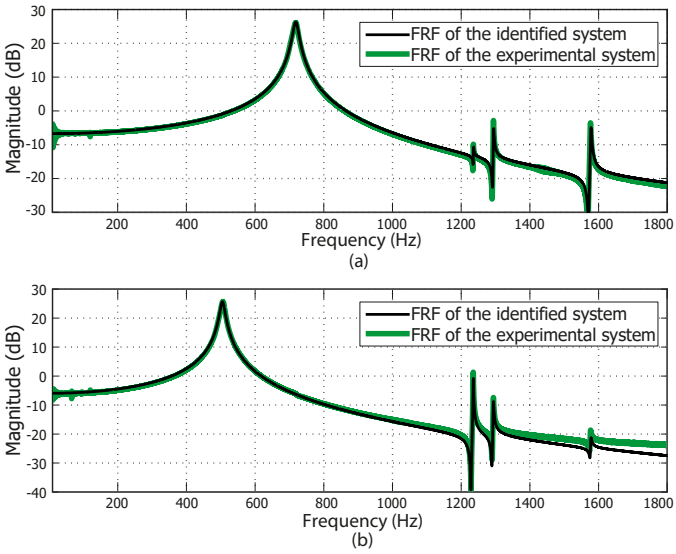

Fig. 2. (a) FRF of the $x-$axis and (b) FRF of the $y-$axis of the experimental platform

TABLE I
PARAMETERS OF THE NANOPOSITIONER

X axis			
Mode	Gain	Damping	Frequency (rad/s)
1^{st}	$\sigma_1 = 3200$	$\zeta_1 = 0.011$	$\omega_1 = 716.2 \cdot 2\pi$
2^{nd}	$\sigma_2 = 250$	$\zeta_2 = 0.0008$	$\omega_2 = 1294 \cdot 2\pi$
3^{rd}	$\sigma_3 = 350$	$\zeta_3 = 0.0008$	$\omega_3 = 1578 \cdot 2\pi$
4^{th}	$\sigma_4 = 800$	$\zeta_4 = 0.0001$	$\omega_4 = 2325 \cdot 2\pi$
Y axis			
Mode	Gain	Damping	Frequency (rad/s)
1^{st}	$\sigma_1 = 2250$	$\zeta_1 = 0.013$	$\omega_1 = 505 \cdot 2\pi$
2^{nd}	$\sigma_2 = 250$	$\zeta_2 = 0.0005$	$\omega_2 = 1235 \cdot 2\pi$
3^{rd}	$\sigma_3 = 100$	$\zeta_3 = 0.0008$	$\omega_3 = 1578 \cdot 2\pi$
4^{th}	$\sigma_4 = 400$	$\zeta_4 = 0.0001$	$\omega_4 = 2325 \cdot 2\pi$

Subsection IV-A, simulations are carried out to illustrate the accuracy, small convergence time of the estimator and the effectiveness of the convergence criterion given by (14). Consequently, the experimental setup is utilized to validate the efficacy of the proposed technique using a practical application in Subsection IV-B. Results provided by the algebraic estimator are used to automatically tune the parameters of the Integral Resonant Controller (IRC) applied to impart damping to the first resonant mode of the nanopositioner axis (inner loop) as well as the integral controller gain (outer loop) that enforces reference tracking, [12]. It is experimentally demonstrated that the proposed method is capable of tracking step-wise changes in the parameters of the system and provides real-time estimations which can be used to perform online automatic tuning of classical control schemes typically employed in nanopositioning systems, thus improving their performance.

A. Simulated results

The most popular trajectory nanopositioners are forced to follow is a raster pattern. This is generated by moving one axis of the nanopositioner in a triangular trajectory and the other in a stair-case trajectory. First, the identified model of the nanopositioner is utilized to simulate the response of the system to the two inputs: step and triangular signals. Later, using the the open-loop response of the system, the performance of the algebraic estimator in correctly estimating the parameters of the system is studied. To highlight the contribution of this article and the advantages of the application of algebraic parameter estimation to a practical system, the relationship between the maximum achievable bandwidth (considering the $\pm$3dB criterion) and the variation in the resonant frequency of the nanopositioner axis are studied under two operating scenarios: (i) Nominal operation -The IRC-based control scheme is pre-tuned to the parameters of the unloaded nanopositioner and (ii) Online algebraic estimation and tuning: The IRC-based control scheme is tuned online using the system parameter estimates obtained via the adopted algebraic estimation technique.

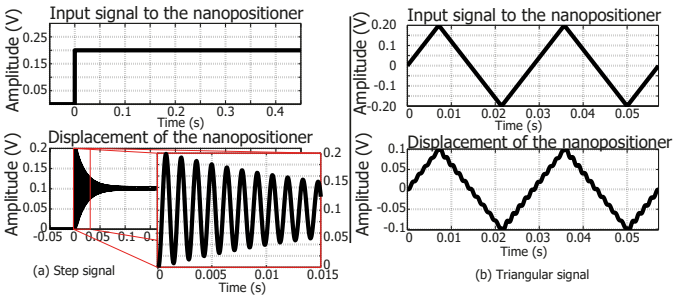

Fig. 3. Input signals applied to the simulated model of the nanopositioner and displacement produced

1) Response to triangular and step signals: Both the step and the triangular inputs have an amplitude of 0.2 V. The triangular input trajectory used to simulate the response of the system has a frequency of 35 Hz, see Figure 3. The step response clearly shows high-frequency oscillations caused by the excitation of the first resonant mode of the system. These oscillations are utilized by the algebraic estimator to identify the parameters of the nanopositioner and, since the step signal produces oscillations with a higher amplitude than those produced by the triangular signal [1], the step signal leads to estimates quicker than the triangular signal.

In order to illustrate the working principle of the proposed method and demonstrate its fast convergence capabilities, Figure 4 shows the displacement of the nanopositioner when excited by the aforementioned step signal. The evolution of the estimation of the natural frequency of the system and a comparison between the evolution of the re-initiation condition $S_n(\omega_n)/|Z_n(\omega_n)|$ and the re-initiation condition proposed in [17] (possibly the most efficient of the conditions proposed in literature for algebraic estimators) are also presented. It is clear that the estimation of ω_n converges very quickly to its actual value, and that the convergence criterion is a monotonically decreasing function which tends to zero (a feature not achieved with the condition proposed in [17]). Note that the limit

[1] This is because the amplitude of the harmonic frequency component that excites the system resonance is higher in the step signal than in the triangular signal.

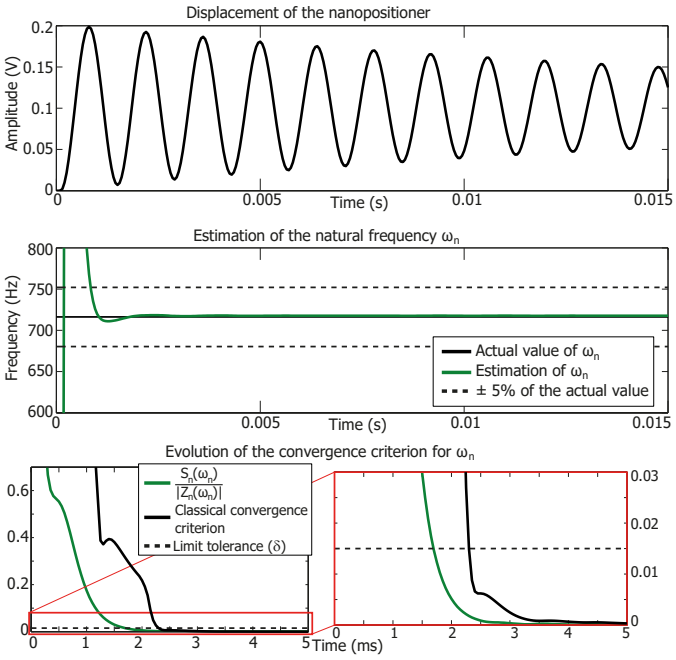

Fig. 4. Displacement of the simulated model of the nanopositioner when excited with a step signal. Evolution of the estimation of the natural frequency of the system over time, and evolution of the stop criterion

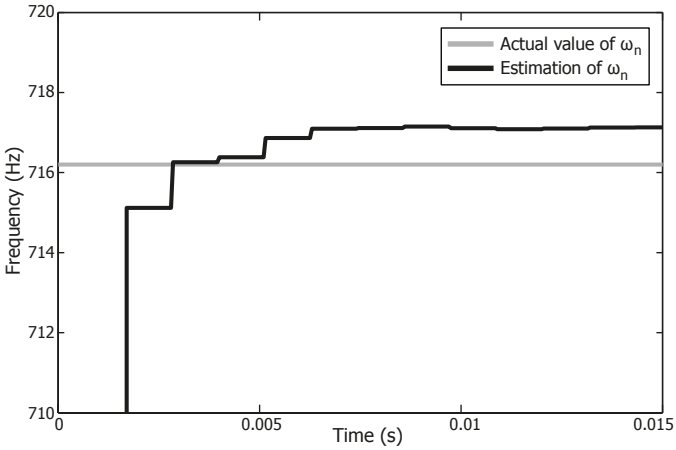

Fig. 5. Estimation of the natural frequency of the system excited by a step input signal.

tolerance δ is reached in a very short time, and thus the condition (14) is verified. Consequently, the estimate of the natural frequency is produced in less than one cycle of the high-frequency oscillations experienced by the system. The evolution of the estimator in the case of a triangular signal is omitted because it presents a similar behaviour but with slightly slower convergence.

Once the efficacy of the algebraic estimator and the convergence criterion are verified, the complete procedure (including the re-initiation step) is analyzed. In this case, the maximum time required to produce a valid estimation T_r is set to 0.015 s. The resulting estimates can be seen in Figure 5. Table II gives a comparison of the estimates produced by the algorithm for both step and triangular inputs.

Because the exact values of the parameters ω_n, σ and ζ are

TABLE II
QUANTIFYING ESTIMATOR PERFORMANCE

Step input

Parameter	Min. Value	Average Value	Max. Value	Standard deviation
ω_n	0.02 (%)	0.11 (%)	0.24 (%)	0.028 (%)
σ	0.067 (%)	0.23 (%)	0.43 (%)	0.052 (%)
ζ	2.01 (%)	14.76 (%)	17.67 (%)	3.28 (%)
Operation time interval (s)	0.00105	0.00106	0.00165	$8.24{\cdot}10^{-5}$

Triangular input

Parameter	Min. Value	Average Value	Max. Value	Standard deviation
ω_n	0.03(%)	0.62 (%)	2.30 (%)	0.63 (%)
σ	0.02 (%)	0.75 (%)	2.66 (%)	0.74 (%)
ζ	16.35 (%)	17.79 (%)	18.53 (%)	0.59 (%)
Operation time interval (s)	0.00105	0.00109	0.0033	0.00031

known in the simulation, the performance of the estimates is expressed in terms of relative error with regards to the actual values of the parameters of the system. As several estimates have been produced in each experiment (because every time the estimator is re-initiated, a new estimate is produced), the minimum, maximum and average errors are shown along with the standard deviation of the errors of the estimation of each parameter. The last index which is utilized to describe the performance of the estimator is the time required to generate each estimate. In each case, the maximum value corresponds to the time taken to produce the first estimate in each case. The time taken for the succeeding estimates is considerably shorter. Additionally, it can be seen that estimates derived with triangular input excitation constitute a larger error compared to those generated via step excitation. This is because of the smaller magnitude of high-frequency oscillations produced by the triangular signal. However, in both cases, the estimates of ω_n and σ (which are the most important parameters required for the correct tuning of any control scheme) present an estimation error less than $\%3$.

2) Performance quantification in closed-loop: To demonstrate the efficacy and performance improvement facilitated by the proposed algebraic estimation with online tuning of control parameters, the proposed technique was compared with the traditional closed-loop approach where the controller parameters are pre-tuned for the nominal unloaded case. For both the traditional pre-tuned and the proposed online-tuned cases, the resonant mode frequency of the nanopositioner axis was reduced to simulate loading and the standard ± 3 dB criterion was used a performance metric. In both cases, the control scheme used was an inner-loop Integral Resonant Controller for damping and an outer-loop integral controller for tracking. Note that for the traditional pre-tuned case, closed-loop performance in the presence of variation in system parameters (resonance frequency and damping coefficient in this case) is solely dependent on the inherent robustness properties of the adopted control scheme. The simulation results are shown in Figure 6.

As seen in Figure 6 (a), for the traditional pre-tuned case, the

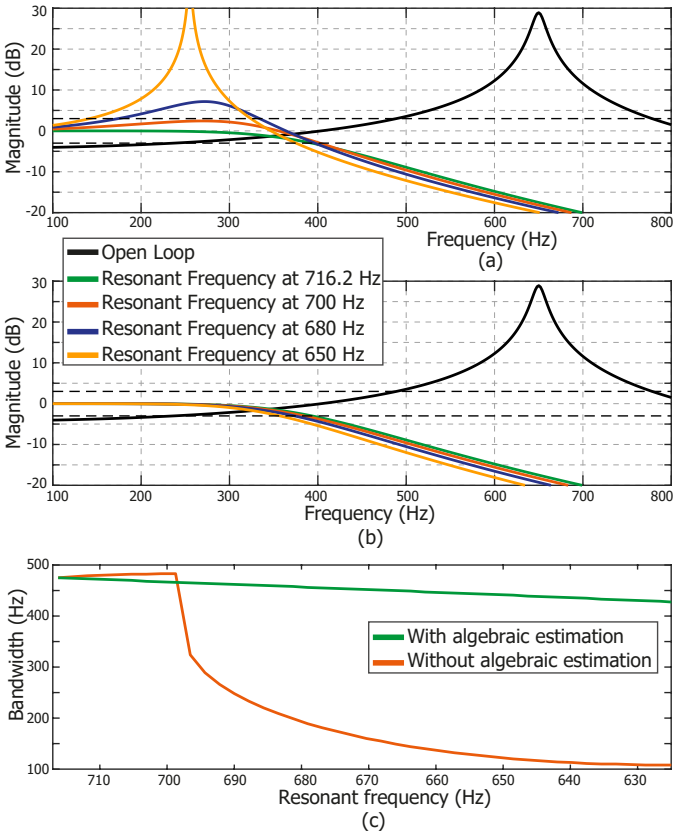

Fig. 6. Open- and closed-loop FRFs of a nanopositioner axis incorporating an IRC scheme with integral tracking designed using the (a) Traditional pre-tuned approach and, (b) Proposed algebraic estimation with online tuning of controller parameters (c) Relationship between closed-loop bandwidth and resonant frequency of the system for the traditional and proposed approaches.

shape of the closed-loop FRF and therefore the resulting 3 dB bandwidth varies substantially and degrades rapidly as the resonant frequency moves away from the nominal unloaded case. The deterioration in the closed-loop bandwidth is clearly seen in Figure 6 (c). On the other hand, as the proposed scheme first estimates the system parameters (resonance frequency and the damping coefficient (ω_n and ζ) and then tunes the controller gains for every resonance frequency shift individually, the loss of bandwidth is more graceful and gradual when compared with the traditional pre-tuned case. This is evident from the FRF's presented in Figure 6 (b) as well as from the bandwidth vs resonance frequency plot given in Figure 6 (c).

B. Experimental results

As gleaned from the simulations, the worst case scenario for the algebraic estimator is the utilization of a triangular input signal, as it produces parameter estimates with larger average errors and requires a longer time to produce them. Therefore, to rigorously interrogate the effectiveness of the proposed scheme and demonstrate its potential for practical application, the worst-case, i.e., employing a triangular signal for procuring parameter estimates, was chosen. It is obvious that the step signal input will result in more accurate estimates and improved estimator performance.

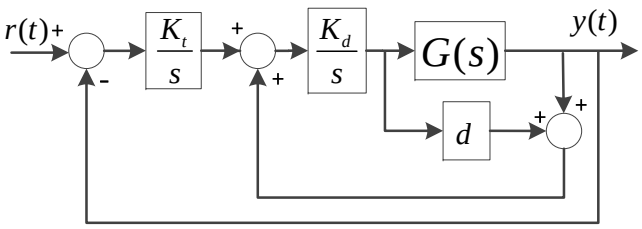

Fig. 7. Block diagram of the IRC control scheme combining both damping and tracking actions.

In this section, the estimates produced by the algebraic estimator are utilized to tune the parameters of the IRC-based damping combined with Integral tracking, see Fig. 7. The three controller parameters that require tuning are: (i) The tracking gain - K_t, (ii) The damping gain - K_d, and (iii) The feed-through term - d. The appropriate values of these parameters are computed online using formulas provided in [34] viz:

$$\begin{aligned} \alpha &= \sqrt{2^{3/2}+4}, \qquad \beta = \sqrt{2}+2 \\ \omega_d &= \frac{\omega_n \alpha \zeta + \omega_n \sqrt{(\alpha^2 - 4\beta)\zeta^2 + \beta}}{\beta} \\ K_d &= \frac{-2\alpha\zeta\omega_d^3 + \omega_n \beta \omega_d^2 - \omega_n^3}{2\zeta\sigma^2} \\ d &= \frac{\beta\sigma^2\omega_d^2 - \omega_n^2\sigma^2}{2\omega_n\alpha\zeta\omega_d^3 - \omega_n^2\beta\omega_d^2 + \omega_n^4} \\ K_t &= \frac{2\zeta\omega_d^4}{\omega_n\beta\omega_d^2 - 2\alpha\zeta\omega_d^3 - \omega_n^3} \end{aligned} \tag{16}$$

These equations aim to place the closed-loop poles of the controlled system in a low-pass Butterworth pattern whose cutoff frequency corresponds to ω_d. It can be seen that the design of the three parameters of the controller depends on the numerical values of the first resonant mode frequency ω_n, the damping coefficient ζ and the dc gain factor σ. As these design rules place the closed-loop poles of the system in very definite positions, any change in the parameters of the nanopositioner would lead to a displacement of the closed-loop poles of the system and thus a degradation of the system's performance, which in extreme cases may lead to instability.

To demonstrate the effectiveness of the proposed algorithm, two scenarios are tested experimentally. In *C*ase 1, assuming no previous knowledge of the system, the estimator first generates parameter estimates using the output of the nanopositioner axis under triangular wave excitation and then uses these estimates to tune the parameters of the IRC control scheme. In *C*ase 2 the nanopositioner is assumed to be operating under nominal conditions and a sudden change in system parameters is introduced via loading. The proposed algorithm is tasked with re-estimating the new system parameters and consequently tuning the control scheme parameters appropriately. To ensue that the proposed scheme works under all possible scenarios of parameter changes, *C*ase 2 is further split into two sub-cases: (a) Payload is increased and (b) Payload is decreased.

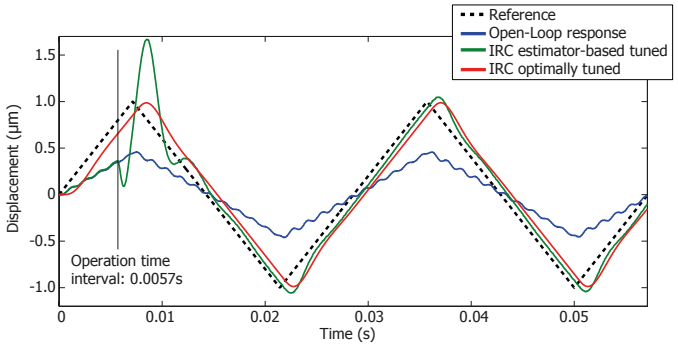

Fig. 8. Evolution of the estimates of the resonance frequency when the experimental system is excited with a triangular signal of 35 Hz. The time at which the algebraic estimator converges is indicated in the figure.

1) Case1: Parameter estimation and control scheme tuning without prior system knowledge: In this experiment, the X-axis of the nanopositioner is excited in open-loop with a triangular signal. The algebraic estimator is initialized to estimate the parameters of the system and the obtained estimates are given as inputs to the design rules of the IRC-based control scheme (16) (it is important to note that all this is done online and autonomously). Finally, once the parameters of the control scheme have been computed, the control scheme is applied to the system to enforce low-error reference tracking. For comparison, the experimental results obtained with this procedure and the experimental results obtained when the control scheme is designed knowing the identified parameters of the system (pre-tuned IRC scheme) are presented in Fig. 8. The open-loop response of the system and the time needed to produce the parameter estimates are also included.

It was noticed that when the re-initiation was triggered in this experiment after the first estimation, the design of the regulator was so effective that the displacement produced by the closed-loop system presents very small oscillations due to the dominant resonant mode. Thus, the estimator was unable to produce any further estimate (it was not able to fulfill (14) in a time T_r=0.015 s).

2) Case 2 : Online tuning of the IRC scheme when payload is increased (Resonance frequency decreases): This experiment was carried out as follows: The parameters of the X-axis of the nanopositioner are used to design the IRC-based control scheme by using (16). The resulting control scheme is then applied to the Y-axis and a 35 Hz triangular signal is used as the reference input. As seen from Table I and Fig. 2, the Y-axis has a much lower resonance frequency (505 Hz) compared to the X-axis (716 Hz) and therefore, this procedure effectively mimics a real-life scenario where a payload is added to the nanopositioner. Subsequently, the algebraic estimator is triggered to estimate the parameters of the Y-axis and re-tune the parameters of the control scheme in order to improve its performance.

The experimental results obtained with the nominal, pre-tuned IRC for the higher resonance frequency, the IRC designed using the proposed online-tuning scheme and the IRC pre-tuned for the correct (reduced) resonance frequency are contrasted in Fig. 9. It is clear that after the operation time

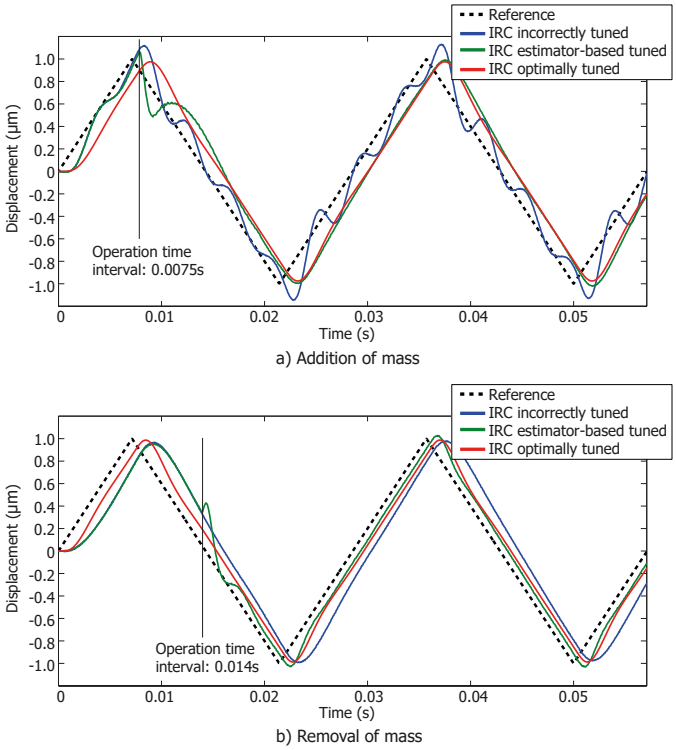

Fig. 9. Displacement of the nanopositioner before and after the estimation procedure in the case of (a) Increase in payload (decrease in resonance frequency) and b) Decrease in payload (increase in resonance frequency). The operation time when the algebraic estimator has converged is clearly indicated.

interval (time required for generating parameter estimates), the consequently tuned IRC-based scheme delivers performance almost matching the one delivered by the optimally tuned one.

It was also noted that after the first estimation, the closed-loop system presents very small oscillations and the estimator was unable to produce any further estimates.

3) Case 3 : Online tuning of the IRC scheme when payload is decreased (Resonance frequency increases): This last experiment aims to mimic the removal of the payload from a nanopositioner that is working with a control scheme designed to operate with the payload (appropriate resonance frequency). The same reasoning as in the previous case is applied, but in reverse. In this case, parameters of the Y-axis of the nanopositioner are first used to design the IRC-based control scheme by using (16), then this control scheme is applied to the X-axis and tracking performance is ascertained using the same 35 Hz triangular trajectory. The algebraic estimator is triggered to estimate the parameters of the X axis and to redesign the parameters of the controller in order to improve its performance. The experimental results obtained are shown in Fig. 9. It is important to note that in this case, the algebraic estimator needs a longer time interval to produce the estimates of the parameters of the system than in the case of addition of payload. This is because a removal of the payload of the system leads to smaller residual vibrations in the tracking of reference signals due to increase in resonance frequency and the lower amplitude of the relevant harmonic component in the triangular trajectory that excites it.

TABLE III
PERFORMANCE COMPARISON

Quantifying algebraic estimator performance

Case	ω_n error	σ error	ζ error
Without previous knowledge	4.63%	7.8%	174%
Increased payload	1.45%	5.22%	180%
Decreased payload	30.51%	33.36%	150%

Quantifying controller estimator performance

	IRC estimator-based tuned		IRC incorrectly tuned	
Index	Payload↑	Payload↓	Payload↑	Payload↓
ISE:	0.00009	0.00006	0.0016	0.00046
IAE:	0.0015	0.0012	0.0058	0.0034
ITAE:	0.00002	0.00001	0.00008	0.00005

4) Performance of the proposed algorithm: The experimental results obtained in the three aforementioned cases, i.e. no previous knowledge of the system, addition of mass and, removal of mass are summarized in Table III. This table quantify on the one hand the performance of the algebraic estimator, by presenting the errors in the estimates of the three parameters of the system, i.e. ω_n, σ and ζ, and on the other hand, compares the performance of the classical IRC scheme versus the proposed algorithm in the tracking of a triangular signal. In order to compare these two schemes, the classical measures of controlled system performance are utilized, i.e. integral squared error (ISE), integral absolute error (IAE) and integral time-weighted absolute error (ITAE). It is important to note that in this case, the goal was not to track the triangular signal without error, but to reproduce the tracking capabilities of the IRC scheme designed by considering a perfect knowledge of the parameters of the system, this is why the different error indexes are computed considering the difference with the signal produced by the IRC optimally tuned.

It can be seen from the data presented in Table III that the proposed control scheme produces very accurate estimates of the parameters of the system and, therefore leads to a tuning of the IRC that is very closed to the case with complete knowledge of the parameters of the system, thus producing much better control performance when compared with the traditional IRC without automatic tunning.

V. CONCLUSIONS

The algebraic framework for the full parametric identification of lightly damped second-order systems is expounded and further combined with a suitable re-initiation algorithm to enable the generation of accurate parameter estimates within one period of the resonance frequency. Simulations as well as experiments carried out on a nanopositioner validate the efficacy of the proposed technique. Closed-loop tracking results obtained via the proposed online estimation and consequent control scheme tuning are in good agreement with those obtained via an optimally tuned control scheme and clearly outperform the static pre-tuned control scheme in presence of parametric variations. This is demonstrated by using the popular and simple IRC-based control scheme implemented on a serial-kinematic XY nanopositioner forced to track typical triangular trajectories. Future research directions include increasing the number of system parameters that can be estimated, investigating methods to reduce estimation errors and incorporating automatic optimal tuning of more evolved control schemes.

REFERENCES

[1] E. Avci, K. Ohara, C. N. Nguyen, C. Theeravithayangkura, M. Kojima, T. Tanikawa, Y. Mae, and T. Arai, "High-speed automated manipulation of microobjects using a two-fingered microhand," *IEEE Transactions on Industrial Electronics*, vol. 62, no. 2, pp. 1070–1079, Feb. 2015.

[2] T. Uchihashi, H. Watanabe, S. Fukuda, M. Shibata, and T. Ando, "Functional extension of high-speed AFM for wider biological applications," *Ultramicroscopy*, vol. 160, pp. 182 – 196, 2016.

[3] K. Yoshida, K. Tanaka, T. Tsujimura, and Y. Azuma, "Assisted focus adjustment for free space optics system coupling single-mode optical fibers," *IEEE Transactions on Industrial Electronics*, vol. 60, no. 11, pp. 5306–5314, Nov. 2013.

[4] D. Min, M. A. Arbing, R. E. Jefferson, and J. U. Bowie, "A simple DNA handle attachment method for single molecule mechanical manipulation experiments," *Protein Science*, vol. 25, no. 8, pp. 1535–1544, 2016.

[5] C. Hyun, H. Kaur, T. Huang, and J. Li, "A tip-attached tuning fork sensor for the control of DNA translocation through a nanopore," *Review of Scientific Instruments*, vol. 88, no. 2, p. 025001, 2017.

[6] A. Fleming, *Design, Modeling and Control of Nanopositioning Systems*, ser. Advances in industrial control. Springer, 2014.

[7] S. O. R. Moheimani, "Invited review article: Accurate and fast nanopositioning with piezoelectric tube scanners: Emerging trends and future challenges," *Review of Scientific Instruments*, vol. 79, no. 7, 2008.

[8] A. J. Fleming, S. S. Aphale, and S. O. R. Moheimani, "A new method for robust damping and tracking control of scanning probe microscope positioning stages," *IEEE Transactions on Nanotechnology*, vol. 9, no. 4, pp. 438–448, Jul. 2010.

[9] Z. Feng, J. Ling, M. Ming, and X. Xiao, "Data-driven feedforward decoupling filter design for parallel nanopositioning stages," in *International Conference on Intelligent Robotics and Applications*, pp. 709–720. Springer, 2016.

[10] M. Mahmoodi, J. K. Mills, and B. Benhabib, "A modified integral resonant control scheme for vibration suppression of parallel kinematic mechanisms with flexible links," *International Journal of Mechatronics and Automation*, vol. 5, no. 1, pp. 44–57, 2015.

[11] A. Sebastian and S. Salapaka, "Design methodologies for robust nanopositioning," *IEEE Trans. Control Syst. Technol.*, vol. 13, no. 6, pp. 868–876, Nov. 2005.

[12] S. S. Aphale, A. Ferreira, and S. R. Moheimani, "A robust loop-shaping approach to fast and accurate nanopositioning," *Sensors and Actuators A: Physical*, vol. 204, pp. 88 – 96, 2013.

[13] S. K. Das, H. R. Pota, and I. R. Petersen, "Damping controller design for nanopositioners: A mixed passivity, negative-imaginary, and small-gain approach," *IEEE/ASME Transactions on Mechatronics*, vol. 20, no. 1, pp. 416–426, Feb. 2015.

[14] S. K. Das, H. R. Pota, and I. R. Petersen, "Multivariable negative-imaginary controller design for damping and cross coupling reduction of nanopositioners: A reference model matching approach," *IEEE/ASME Transactions on Mechatronics*, vol. 20, no. 6, pp. 3123–3134, Dec. 2015.

[15] S. K. Das, O. U. Rehman, H. R. Pota, and I. R. Petersen, "Minimax LQG controller design for nanopositioners," in *Control Conference (ECC), 2014 European*, pp. 1933–1938, Jun. 2014.

[16] M. Fliess and H. SiraRamrez, "An algebraic framework for linear identification," *ESAIM: COCV*, vol. 9, pp. 151–168, 2003.

[17] E. Pereira, J. R. Trapero, I. M. Daz, and V. Feliu, "Algebraic identification of the first two natural frequencies of flexible-beam-like structures," *Mechanical Systems and Signal Processing*, vol. 25, no. 7, pp. 2324 – 2335, 2011.

[18] E. Pereira, J. Trapero, I. Daz, and V. Feliu, "Adaptive input shaping for manoeuvring flexible structures using an algebraic identification technique," *Automatica*, vol. 45, no. 4, pp. 1046 – 1051, 2009.

[19] J. C. Cambera, A. San-Millan, and V. Feliu-Batlle, "Payload mass identification of a single-link flexible arm moving under gravity: An algebraic identification approach," *Shock and Vibration*, p. 13, 2015.

[20] Y. Tian, B. Shirinzadeh, and D. Zhang, "A flexure-based mechanism and control methodology for ultra-precision turning operation," *Precision Engineering*, vol. 33, no. 2, pp. 160 – 166, 2009.

[21] M. Karimi-Ghartemani, H. Karimi, and M. R. Iravani, "A magnitude/phase-locked loop system based on estimation of frequency and in-phase/quadrature-phase amplitudes," *IEEE Transactions on Industrial Electronics*, vol. 51, no. 2, pp. 511–517, Apr. 2004.
[22] M. Mojiri and A. R. Bakhshai, "An adaptive notch filter for frequency estimation of a periodic signal," *IEEE Transactions on Automatic Control*, vol. 49, no. 2, pp. 314–318, Feb. 2004.
[23] M. Hou, "Amplitude and frequency estimator of a sinusoid," *IEEE Transactions on Automatic Control*, vol. 50, no. 6, pp. 855–858, Jun. 2005.
[24] G. Fedele and A. Ferrise, "Non adaptive second-order generalized integrator for identification of a biased sinusoidal signal," *IEEE Transactions on Automatic Control*, vol. 57, no. 7, pp. 1838–1842, Jul. 2012.
[25] G. Fedele and A. Ferrise, "A frequency-locked-loop filter for biased multi-sinusoidal estimation," *IEEE Transactions on Signal Processing*, vol. 62, no. 5, pp. 1125–1134, Mar. 2014.
[26] M. R. Osborne and G. K. Smyth, "A modified prony algorithm for exponential function fitting," *SIAM Journal on Scientific Computing*, vol. 16, no. 1, pp. 119–138, 1995.
[27] J. R. Trapero, H. Sira-Ramrez, and V. F. Batlle, "A fast on-line frequency estimator of lightly damped vibrations in flexible structures," *Journal of Sound and Vibration*, vol. 307, no. 1, pp. 365 – 378, 2007.
[28] A. San-Millan and V. Feliu, "A fast online estimator of the two main vibration modes of flexible structures from biased and noisy measurements," *IEEE/ASME Transactions on Mechatronics*, vol. 20, no. 1, pp. 93–104, Feb. 2015.
[29] J. Cortes-Romero, C. Garcia-Rodriguez, A. Luviano-Juarez, and H. Sira-Ramirez, "Algebraic parameter identification for induction motors," in *IECON 2011 - 37th Annual Conference on IEEE Industrial Electronics Society*, pp. 1734–1740. IEEE, Nov. 2011.
[30] R. Garrido and A. Concha, "An algebraic recursive method for parameter identification of a servo model," *IEEE/ASME Transactions on Mechatronics*, vol. 18, no. 5, pp. 1572–1580, Oct. 2013.
[31] G. Mamani, J. Becedas, V. FeliuBatlle, and H. SiraRamrez, "Open- and closed-loop algebraic identification method for adaptive control of DC motors," *International Journal of Adaptive Control and Signal Processing*, vol. 23, no. 12, pp. 1097–1103, Mar. 2009.
[32] J. Mikusinski and T. Boehme, *Operational Calculus*, ser. 2nd ed., vol. I. New York: Pergamon, 1987.
[33] S. E. R. L. Allison Jones, Charles W. Champ, "The performance of exponentially weighted moving average charts with estimated parameters," *Technometrics*, vol. 43, no. 2, pp. 156–167, 2001.
[34] D. Russell, A. J. Fleming, and S. S. Aphale, "Simultaneous optimization of damping and tracking controller parameters via selective pole placement for enhanced positioning bandwidth of nanopositioners," *Journal of Dynamic Systems, Measurement, and Control*, vol. 137, no. 10, pp. 101 004–101 012, Jul. 2015.